

ASVA 97

2-4 April 1997 Tokyo, Japan

ANALYSIS OF THE TRIGGERING DELAY IN A STRING BOWED TO ANOMALOUS LOW FREQUENCIES

Knut Guettler

*The Norwegian State Academy of Music
P.B. 5190 Majorstua, 0302 Oslo - Norway
E-mail: knut.guettler@samson.mnh.no*

ABSTRACT

The desire to expand the frequency range of a bowed instrument below the fundamental frequency of the lowest sounding string, has led to some interesting practical applications. Such notes, being carefully bowed with low velocity in combination with high bow force, depend on a periodic triggering of slip-stick caused by waves other than the normal "Helmholtz corner". Their frequencies are not usually true "subharmonics", since they are not simply related to the natural first-mode frequency of the system. The triggering is often determined by a combination of transverse and torsional waves and their respective reflections at the endpoints of the string. Computer simulations of the bowed string reveal which frequencies are obtainable through this bowing technique and how the triggering comes about. Both the bowing position and the torsional wave velocity influence the possible length of periods.

INTRODUCTION

In the CASA Symposium on Musical Acoustics, Annapolis 1991[1], Roger Hansson and Oliver Rodgers demonstrated the phenomenon of Anomalous Low Frequencies (ALF) performed on the viola. Motion patterns of different points along the string gave insight in the nature of some of these signals, while others were more difficult to interpret. The present author had come across these peculiar oscillations at two earlier occasions: the first in a summer course for string bassists in Cincinnati, Ohio 1979, where one student showed his ability to play notes far below the normal range of his instrument. Secondly, through his own computer simulations of the bowed string. In 1993 an appointment between Hanson, the present author and the editor of the CAS Journal was made as to make two accompanying analyses of the phenomenon in two joint articles. These were printed November 1994 [2][3]. Most of the content of the present article has been derived from the CASJ article [3]. For more comprehensive information on simulation parameters etc., the reader should refer to this one.

ON THE SIMULATION TECHNIQUE

In order to understand the slip-stick triggering mechanism involved, a computer program able to simulate transverse and torsional movements of the string has been employed. The programmable parameters are: wave impedances and velocities, reflection functions, bow compliance, bow velocity and "pressure" as functions of time, and their interaction with a hyperbolic friction characteristic of the resin. The program, as well as the present analysis, is based on D'Alembert's solution [4] to the wave equation, where the positions of waves moving in opposite directions are shifted with time. The solution in the continuous form reads:

$$(1) \quad \eta(x, t) = \eta_+(x-ct) + \eta_-(x+ct)$$

where $\eta_{(\pm)}$ = (partial) string displacement; c = the propagating speed of the wave; x = position on the string; t = time. Two sets of eq. (1) are used: one for transverse- and one for torsional waves. In the simulation program, these interact only at the point of bowing, and only through frictional force. Dispersion and losses are carried out by reflection functions "at the string terminations". In general, the concepts of string simulation developed by McIntyre, Woodhouse and Schumacher [5][6][7][8][9] have been adopted.

Some simulation parameters

To appreciate the influence of the ratio between transverse and torsional wave velocities, two different strings are simulated: for string A, the ratio $\zeta = C_{TRV} / C_{TOR} = 0.300$, and for string B, $\zeta = 0.213$. The Q-values for these strings range between 500 and 1000 for the transverse modes (equal for both strings), while the Q-values for the torsional modes varies between 17 and 65 (7 and 24) for string A (B). The difference between A and B is only due to their propagation-speed differences, as their end reflections as functions of time are kept equal for both strings. The ratio of transverse and torsional wave impedances is set to $\Omega = Z_{TRV} / Z_{TOR} = 0.65$ for both strings to facilitate comparison. The admittance of the (single-pointed) bow is set to zero.

Potential frictional force

The frictional force (f_{ST}) between the non-compliant bow and the string during the *static* intervals may be expressed through the following equation (which can be derived from ref. [8], eqs. (B13) and (B14):

$$(2) \quad f_{ST}(t) = 2Z_{CMB} [V_{BOW} - \sum V_{w(1-4)}(t)]$$

where

Z_{CMB} = the combined wave impedance of the string, i.e., $(Z_{TRV} Z_{TOR}) / (Z_{TRV} + Z_{TOR})$;
 V_{BOW} = velocity of the bow; $v_{w(i)}(t)$ = signal of partial wave(i) arriving at the bow; throughout this paper the term "signal" means derivative of (partial) displacement with respect to time, i.e., $\delta\eta_{(\pm)}(x) / \delta t$. $v_{w1}(t)$ and $v_{w2}(t)$ = *transverse* signals propagating away from the nut and the bridge, respectively; $v_{w3}(t)$ and $v_{w4}(t)$ = *torsional* signals propagating away from the nut and the bridge, respectively.

Torsional signal is to be understood as string radius times radians per second, with the convention that the angle twist is negative when the translational displacement is positive *on a fixed bow holding a static grip*. The sum of the four partial signals (i. e., velocities) gives the *surface velocity* the string would have taken at the point of bowing, if the bow had no friction. It is convenient to refer to f_{ST} as "*potential frictional force*", disregarding whether the friction be static or not. The value of $f_{ST}(t)$ expresses the frictional force that occurs as long as the

limiting (static) frictional force (f_L) is greater than $f_{ST}(t)$. At the very moment $f_L < f_{ST}(t)$, the friction will change from static to sliding. Thus, $f_{ST}(t) - f_L$ expresses the margin for this change to happen, at any instant.

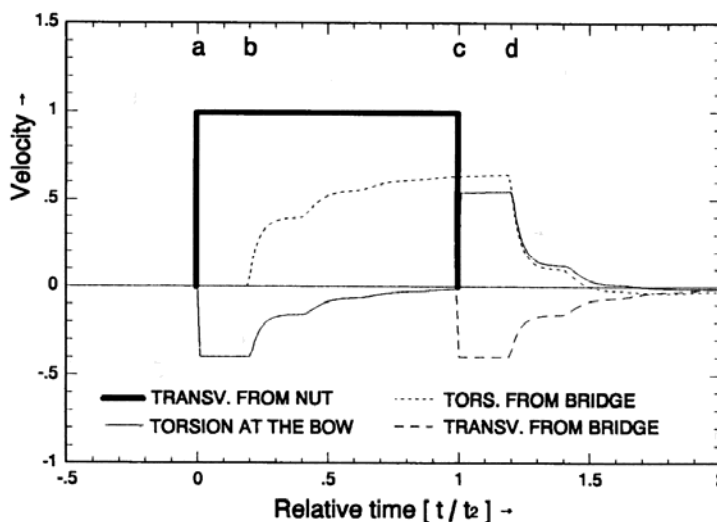
RESPONSES TO A PULSE

To estimate the frictional effects of a pulse rotating both in the transverse and the torsional planes, the following simulations were run: at $t = 0$, the string is released from an initial maximum *transverse* displacement (η) at the point of bowing, with decreasing displacement on both sides toward the bridge and the nut - similar to a pizzicato. (The string is pulled in positive bowing direction at its center: *no torsional displacement*.) During one "normal *slipping* interval of Helmholtz motion"[10], $0 \leq t < t_2$ (where $t_2 = 2bL/C_{TRV}$ and $L =$ string length), there is no contact between the bow and the string. In this interval the string takes the transverse velocity V_{INI} under the bow. At $t \geq t_2$, the a static grip is established between the string and the bow, which now takes the velocity $V_{BOW} = 0.001\eta$ /s. The effect of the bow pulling the (reflecting) string with a constant velocity, is then superimposed on all reflections of V_{INI} , causing the average frictional force to increase with time.

There are certain time spans where a release might take place, provided the limiting static frictional force be low enough. However, there are even larger time spans where release cannot happen, due to the fact that during these, the frictional force "falls in the shadow" of a preceding force peak of a higher value (indicated by horizontal, dashed lines). When comparing the two Figures 1 and 2 (next page), one will appreciate the role of the wave-velocity ratio, ζ , which is the only parameter changed between the two. During a normal Helmholtz movement of the string), the positive peak at $t/T_0 = 1$ will trigger a string release. If the limiting static frictional force is higher than the potential frictional force at $t = T_0$, the release will be delayed until a peak high enough does the trick. The next opportunity of triggering appears with the edge rising to the peak at $t = T_0(1 + \zeta)$, which is equal to $1.300T_0$ for string A, and $1.213T_0$ for B. In both Figures 1 and 2, V_{INI} arrives at the bow at $t_1 = T_0 - t_2$ after the first reflection at the nut.

Figure 3:

We make the simplification that the wave arriving at the bow at t_1 is a transverse unit velocity pulse, t_2 wide: a torsional pulse will build up after several reflections at the bridge. If the unit pulse arrives at $t = t_1$, the torsional pulse will reach its maximum at $T_0 + \zeta t_2$. The impedance ratio (Ω) is 0.65 as for the strings A and B, while the velocity ratio (ζ) in this figure equals 0.200. Certain points of time are marked: $a=t_1$, $b=t_1 + \zeta t_2$, $c=T_0$, $d=T_0 + \zeta t_2$.



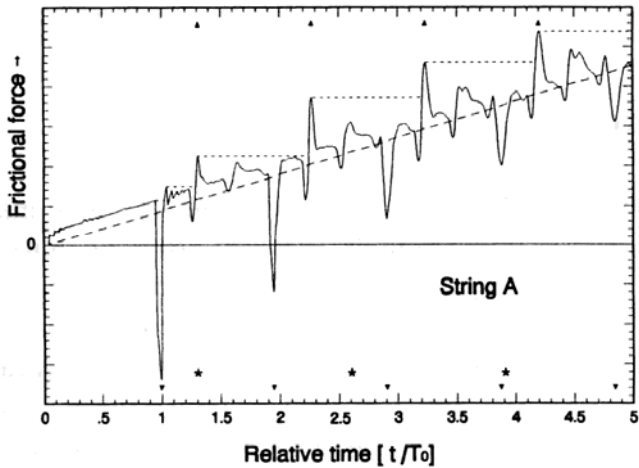


Figure 1:

Frictional force on string A when the reflections of an initial velocity pulse, V_{INI} , are superimposed on the force originating from a bow pulling the string with a fixed velocity (dashed ramp). Force peaks caused by torsional nut reflections occur in intervals of approximately t_l (marked ▲), starting at $t = T_0(1+\zeta)$. These are potential triggers of slipping. The points of time for force reductions (marked ▼) are determined by transverse nut reflections of the initial string fly-back, and occur with the same intervals. Integer multiples of $T_0(1+\zeta)$ are marked *, see text.

Figures 4 a and b:

Waves arriving at the bow (upper graph): waves arriving from the nut are drawn with solid lines, while waves arriving from the bridge are dotted.

Frictional forces (lower graph): when string A is bowed to a normal Helmholtz motion. Spikes of the actual frictional force trigger releases at $t/T_0 = 1, 2, 3$, etc. (With numeric simulation these are not usually recorded as equal to f_L , this value not lasting till the conclusion of the time step; here they are drawn to full height.) The potential frictional force, f_{ST} (dotted) rises high during the slipping periods. The height of f_{ST} above the wavy act. frict. force, determines the bow force tolerance. The dashed horizontal line shows the limiting static frictional force applied for the simulation.

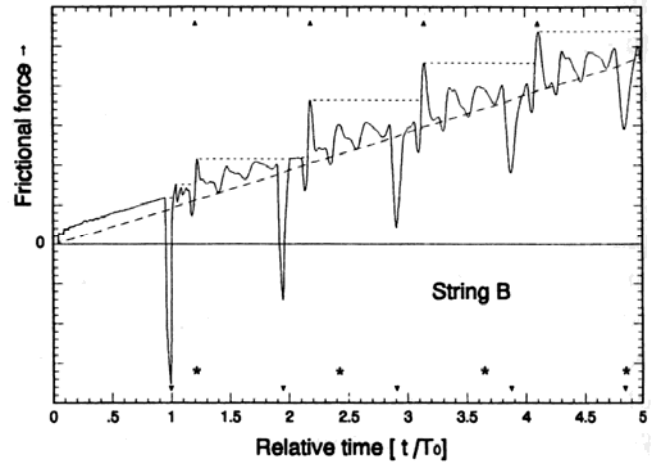
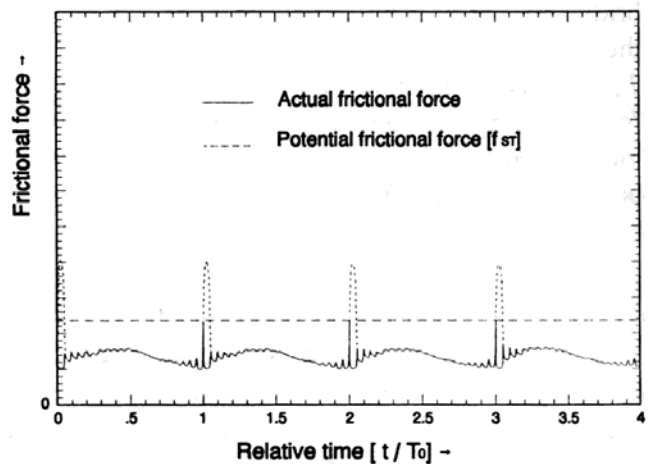
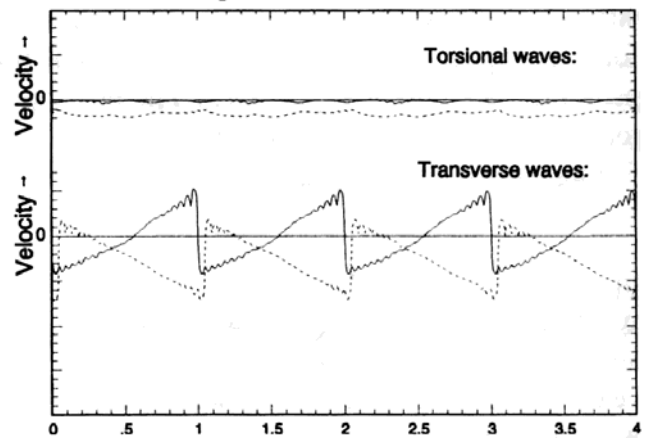


Figure 2:

String B: V_{INI} and the V_{BOW} are the same as for string A in figure 5. Notice how the wave velocity ratio ($\zeta = 0.300$ for string A; $\zeta = 0.213$ for string B) determines the positions of force peaks on the time axis.

String A in Helmholtz motion:



TRIGGERING OF ANOMALOUS LOW FREQUENCIES (ALF)

Torsional triggering

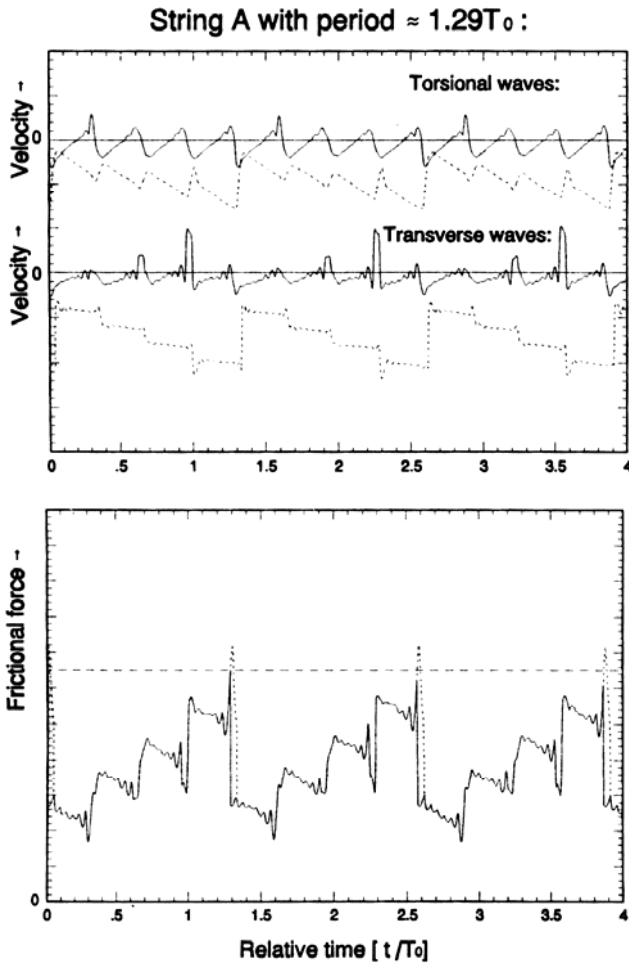
During a steady-state oscillation with delayed releases, the reflections of one string flyback will combine with the fading reflections of the previous string releases. Dependent on the interval between two slips, old and new reflections may combine to powerful peaks of f_{ST} , which ensure stable triggering, or they can lead to cancellation of the same. Figures 5 a and b show how string A forms new fundamental periods, which are stable and prolonged by 29.3%. This is somewhat more than a *major third* step down. For string B (Figures 6 a and b), the prolongation is about 20.4%, corresponding to about a *minor third* down (which seems to be normal for most violin strings). In both cases the triggering is stable, with reasonable "reserves" of f_{ST} , as compared to the limiting static frictional force (dashed horizontal line). Notice that all the figures in this article are drawn to the same scales with respect to their coordinates, for ease of comparison.

The bow force tolerances are less in Figs. 5 and 6 than they are during the Helmholtz motion of Fig. 4. This is due to the partial cancellation that takes place if $nT_0(1+\zeta) \approx (mt_1$ through $mt_1 + t_2)$ (where $n = 1,2,3\dots$ and $m = 1,2,3\dots$). While the left side of this expression indicates integer multiples of the time of the first "torsional force maximum", the right side indicates time spans of "transverse force reductions". In Figs. 1 and 2, torsional maxima and transverse minima are marked \blacktriangle and \blacktriangledown respectively, while integer multiples of $1+\zeta$ are marked *. The width of the force reduction is about t_2 when $m = 1$, but increases with higher values of m , due to dispersion and losses during the reflections. Concerning string A, the "soft cancellation" takes place near the time $t \approx 3.9T_0$ after a string release (i.e., * and \blacktriangledown falling close when $n = 3$, and $m = 4$). For string B, the corresponding values are $t \approx 4.85T_0$; $n = 4$, and $m = 5$. It was noticed during the simulations that cancellation was a greater problem for lower bow velocities than for higher. For example: when string B was bowed with 1/4 of the bow velocity used for Figure 6, the typical sequence of periods would be: $[T_0(1+\zeta)]$, $[T_0(1+\zeta)]$, $[T_0(1+\zeta)]$, $[T_0(1+\zeta+t_1\zeta)]\dots$, with each fourth period additionally prolonged by $t_1\zeta$. This implies that the last triggering is initiated by a torsional wave arriving at the bow *after a second reflection at the nut*.

Due to the nonlinear behavior of the system, as well as the combinations of multiple reflections, it is difficult to give exact equations concerning prolongation, etc. But, from the expressions above, one can derive the following "thumb rules", which may show useful in some practical applications: For a stable, lowered frequency (f_{ALF}) triggered by torsional waves, the approximate wave velocity ratio (ζ) can be found through the equation:

$$(3) \quad \zeta \approx \frac{f_0}{f_{ALF}} - 1; \quad [f_0(1-\beta) > f_{ALF} > \frac{f_0}{2-\beta} = \frac{1}{T_0+t_1}]$$

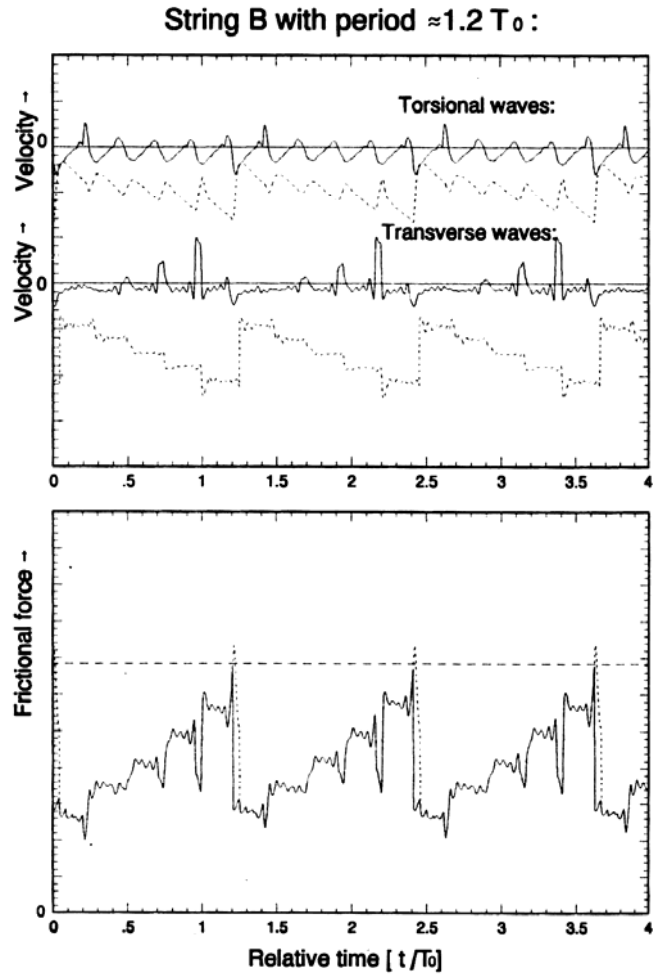
The best estimation of ζ is done if β is small, because then a narrow triggering pulse is created, and triggering bound to happen near to its peak, i.e., near $t = T_0(1+\zeta)$. The frequencies most likely to occur as results of torsional triggering are:

**Figure 5:**

String A: when combining the bow velocity used for the simulations of Fig. 4, with a higher bow force, a prolongation of the periods between slips of approx. 29.3% is obtained.

$$(4) \quad f_{ALF} \approx \frac{1}{T_0(1+\zeta) + nt_1}; \quad (n = 0, 1, 2, \dots; \zeta > \frac{t_2}{t_1})$$

Torsional triggering, as described above, requires an efficient *transformation* between transverse and torsional waves when hitting the bow. The factor of transformation from transverse to torsional velocity at a non-compliant bow is equal to $-Z_{CMB}/Z_{TOR}$, while the *transverse reflection* factor is $-Z_{CMB}/Z_{TRV}$, and the *transmission* coefficient Z_{CMB}/Z_{TOR} . Correspondingly, the transformation from torsional to transverse velocities is equal to $-Z_{CMB}/Z_{TRV}$, and the *torsional reflection* factor equal to $-Z_{CMB}/Z_{TOR}$, while the transmission coefficient is Z_{CMB}/Z_{TRV} . Hence, the chances of achieving a comparatively high, "torsional" f_{ST} increase as the value of Ω approaches unity. During sliding friction, partial signals (transverse and torsional) equal to $f_s/2Z_{TRV}$ and $f_s/2Z_{TOR}$ are superimposed on the partial signals arriving at the bow; " f_s " being the frictional force as function of the *resulting relative velocity* between the string surface and the bow. Equally important are the Q-values of the higher torsional modes, as these determine the shape of the returning pulse and its triggering potential. It is the author's experience that torsional triggering is more easily obtained on the violin than on the double bass, a circumstance which may indicate a difference in the torsional damping.

**Figure 6:**

When combining the bow velocity used for the simulations of Fig. 4, with a higher bow force, a prolongation of the periods between slips of approx. 20.4% is obtained with string B.

String A with period $\approx 2T_0$:

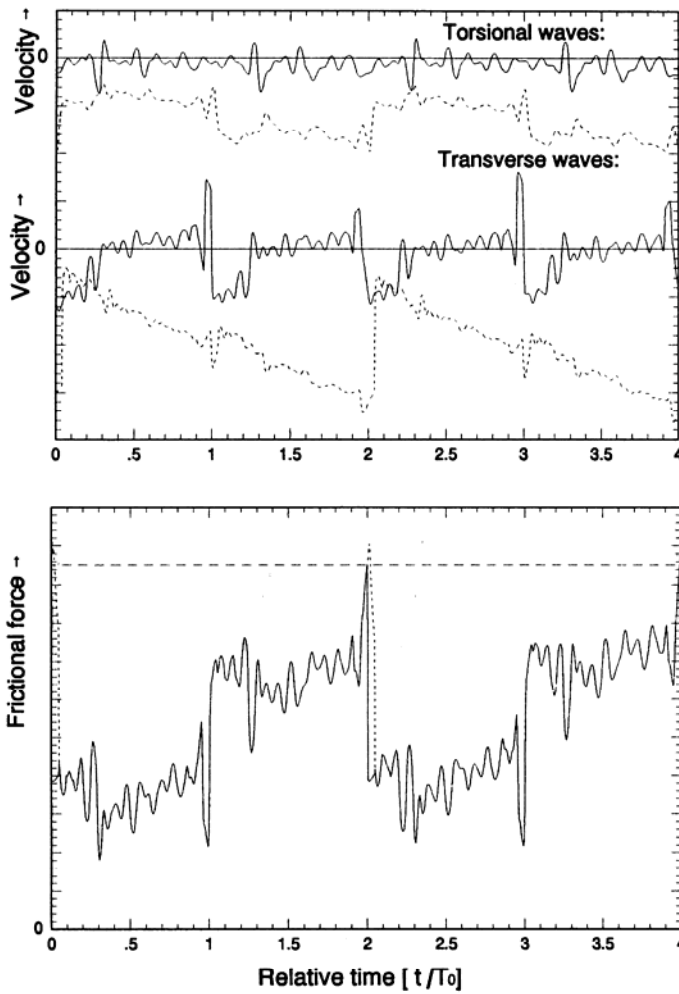


Figure 7: When applying a bow force four times higher than the one used for the Helmholtz motion of Fig. 4, a period prolongation of approx. 100% is obtained. The triggering is here caused by transverse waves after nut reflections, as opposed to the Figures 5 and 6, where torsional waves did the triggering.

Transverse triggering

As can be appreciated from Figures 7 a and b, a transverse wave can trigger a slip when arriving at the bow after one or more reflections at the nut. Similar to eq. (4), a set of possible periods $1/f_{ALF}$ exists, all spaced with intervals of approximately t_1 . However, the increased duration of the force drop, which was mentioned earlier, adds to the period and is indicated as a corrective term, "width", in the equation:

$$(5) \quad f_{ALF} \approx \frac{1}{T_0 + nt_1 + width}; \quad (n = 1,2,3...)$$

One important contributor to this "width" term is the interaction between two reflections experienced by the transverse fly back pulse as it hits the bow when returning after a nut reflection. These two, which appear in quick succession and rejoin in transverse form, are:

- (1) the transverse, immediate reflection at the bow (at $t = 0$) and
- (2) the repeated reflections between the bridge and the bow, consisting of transformed, torsional waves (returning to the bow where they retransform to transverse at $t = \zeta t_2, 2\zeta t_2, 3\zeta t_2, \dots$). Their combined reflection builds up in steps during the static friction. For a non-compliant bow in combination with a bridge totally reflecting transverse and torsional waves, one can estimate a time constant, which outlines the first part of this non-continuous function (see eq. 6, Z_{TOR}/Z_{CMB} being the reciprocal of the transverse transmission coefficient). For bridge reflections including losses, the time constant will be even greater. Notice that an increase of β also implies an increase of the time constant of eq. (6), thus contributing to the wide term and the delay of triggering:

$$(6) \quad R_{CMB}(t) = \exp[-(t+\zeta t_2)/\tau] - 1 \quad (0_+ \leq t < t_2)$$

$$\text{where:} \quad \tau = \frac{\zeta t_2}{\ln(Z_{TOR}/Z_{CMB})}$$

Paths of triggering waves

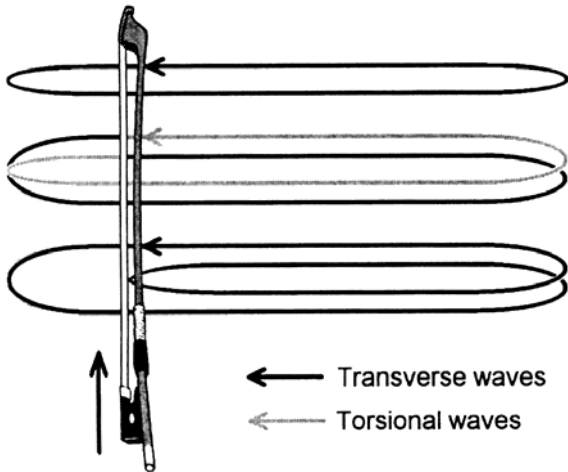


Figure 8:

Basic signal paths for

a) Helmholtz motion, (i.e., triggering at nT_0)

b) Torsional triggering (at $nT_0(1+\zeta)$)

c) Transverse triggering (at $n(T_0+t_1)$).

Other signal paths are possible, but most likely as combinations of a) and one or more of the extra loops of b) and c).

REFERENCES

1. Hanson, R.J., Halgedahl, F.W., and Schneider, A.J., Presentation at CASA-'91 Ninth Annual Symposium on Musical Acoustics, Annapolis, Maryland, U.S.A. 1991 (The first demonstration of ALF was at the ASA mtg in St. Louis in November 1989, where Fred Halgedahl demonstrated on a violin.)
2. Hanson, R.J., Schneider, A.J. and Halgedahl, F.W., "Anomalous Low-Pitched Tones from a Bowed Violin String" CAS Journal, 2, 6(II), 1-7, 1994.
3. Guettler, K., "Wave analysis of a string bowed to anomalous low frequencies", CAS Journal, 2, 6(II), 8-14, 1994. Unfortunately the pages 11, 12 and 13 were printed as 13, 11 and 12 in this publication.
4. The D'Alembert solution is thoroughly explained in Cremer, L., "The Physics of the Violin", The MIT press, London 1983, pages 18-20.
5. McIntyre, M.E. and Woodhouse, J., "On the Fundamentals of Bowed-String Dynamics", Acustica 43 (1979), 93
6. Schumacher, R.T., "Self-Sustained Oscillations of the Bowed String", Acustica 43 (1979) pages 109-120.
7. McIntyre, M.E., Schumacher, R.T., and Woodhouse, J., "Aperiodicity in Bowed-String Motion" Acustica 49 (1981) pages 13-32.
8. McIntyre, M.E., Schumacher, R.T., and Woodhouse, J., "On the oscillations of musical instruments" JASA 74 (1983).
9. A flow chart of the bowed string simulation technique of McIntyre and Woodhouse is presented in Cremer, L., "The Physics of the Violin", The MIT press, London 1983, pages 158-170.
10. Helmholtz, H., "On the Sensation of Tone", Dover, N.Y. (1954) (Orig. German edition: 1877)